Rock Mechanics and Rock Engineering (2021) 54:2697–2705
https://doi.org/10.1007/s00603-021-02434-x

ORIGINAL PAPER

Measuring the Effectiveness and Durability of Silicified Sandstones and Conglomerates from Zamora, Spain Subject to Silico-organic Treatments and/or Freezing/Thawing Processes

A. C. Iñigo[1] · J. García-Talegón[2] · V. Vicente-Palacios[3] · S. Vicente-Tavera[3]

Received: 5 August 2020 / Accepted: 5 March 2021 / Published online: 18 March 2021

Abstract
This work was carried out on fresh samples of silicified sandstone and white conglomerate quarry from Zamora, Spain. The stones were treated with conservation treatments (H224, RC70, and RC80) and/or processes of freeze/thaw aging (similar to that of cold areas). The values obtained for the chromatic coordinates (L*, a*, b*) and the ultrasound propagation speed of the samples studied were analyzed and a statistical design was created. In addition, a multivariate technique (Canonical Biplot) was applied to determine the effectiveness of the treatments and the durability of the fresh and treated stones. In most of the cases studied, the ultrasonic propagation speed decreased in both the untreated samples and those treated with the conservation products after carrying out the aging process. Moreover, it was found that the ultrasonic propagation speed was lower with respect to the treated samples. Our results indicate that the treated samples are more durable than the untreated fresh samples and that the most severe changes can be appreciated when the untreated (fresh) samples are compared with their corresponding treated samples. For these samples, the ultrasonic propagation speed increased showing the effectiveness of each of the conservation products. The most effective consolidating treatment used was RC80. Also, the chromatic coordinates of the treated samples, in general, were darker (↓L *), redder (↑a *), and more yellow (↑b *) with respect to the fresh, untreated quarry samples, except in sample Z1 treated with RC80, where redness (↓a *) and yellowness (↓b *) decrease.

Keywords Silicified rocks · Silico-organic treatments · Effectiveness · Freezing/thawing aging · Durability · Canonical Biplot

1 Introduction

The city of Zamora is located in the autonomous community of *Castilla y León*. This region has a Mediterranean climate with a continental trend, conditions that give rise to the frequently occurring degradation caused by freezing/thawing and cooling/heating processes (García-Talegón et al. 2006, 2013; Iñigo and Vicente-Tavera 2001, 2002; Iñigo et al. 2000; Vicente 1996). To reproduce the climatic effects experienced by this area, a climatic chamber, under controlled conditions, was used to carry out an accelerated freezing/thawing and cooling/heating aging treatment (− 20/110 °C) on fresh quarry samples and quarry samples treated with silico-organic products (Iñigo et al. 2000, 2006).

Determination of the ultrasonic propagation speed allows us to measure the connectivity of different minerals in a specific stone material. When the material is treated with a consolidant, the connectivity between minerals increases (an indication of the effectiveness of the treatment) (El-Gohary 2013), whereas when the materials are subjected to accelerated aging treatments in a climatic chamber under controlled conditions (durability versus processes of freezing/thawing) or when forming part of a monument the ultrasonic propagation speed tends to decrease (Castillo-Oli 2018; Ortiz et al. 2013; Iñigo et al. 2013; Molero et al. 2012; Liu et al. 2012; Ruedrich et al. 2011; Mahmoud et al. 2010; Bellopede and Manfredotti 2006; Minster et al. 2006; Chen et al. 2004; Valdeón et al. 1996; Matsuoka 1990).

✉ A. C. Iñigo
adolfo.inigo@irnasa.csic.es

[1] IRNASA/CSIC de Salamanca, Salamanca, Spain

[2] Departament of Geology, University of Salamanca, Salamanca, Spain

[3] Departament de Statistics, University of Salamanca, Salamanca, Spain

Color is a parameter that should be controlled when quarry stones are used as construction material. This is particularly relevant when stones are subjected to the environmental conditions of an area (Vicente-Palacios et al. 2017; Aparecida-del Lama et al. 2016; Grossi et al. 2015; Grossi and Brimblecombe 2008; Iñigo et al. 2004; Martín et al. 2002; Zezza 2002a, b; Sebastián-Pardo and Zezza, 1998) or after the application of conservation treatments (Pelin et al. 2016; Rivas et al. 2011; Carmona-Quiroga et al. 2010; García et al. 2010; Iñigo et al. 1997), where the effects of such factors on color should be as small as possible.

In this work, a multivariate statistical design was performed using a Canonical Biplot to determine variations in the ultrasound propagation speed in three spatial directions (Vx, Vy, Vz) and the chromatic coordinates (L*, a*, b*). This information was used to determine: (a) the durability of fresh quarried stone after the application of freezing/thawing and cooling/heating processes (− 20/110 °C); (b) the effectiveness of different silico-organic treatments (H224, RC70, and RC80) applied to the fresh quarried stone samples; and (c) the durability after the application of consolidating treatments in combination with the freezing/thawing and cooling/heating accelerated aging (− 20/110 °C).

2 Materials and Methods

One natural siliceous conglomerate (Z1: a white conglomerate) and four siliceous sandstones (TG: thick white sandstone, TB: a white sandstone, TO: an ochre sandstone, and TR: a red sandstone) from Zamora were tested. All were porous and contained strongly reactive components (e.g., swelling clays, opal, etc.) and their origin, mineralogical and chemical composition and petrophysical properties have been described elsewhere (Añorve, 1997). In addition, all of these materials are used in the construction of buildings and are currently being used in the reconstruction of the Cathedral and other buildings in Zamora (Spain).

The following silico-organic products were used to treat the above-mentioned stones: (a) the consolidator RC70 (ethyl silicate); (b) the consolidator and water-repellent RC80 (ethyl silicate, methyl resin, and resinous polysiloxane that is hydrophobic); and (c) the hydrophobic product H224 (alkylpolysiloxane oligomer). The composition of these products does not produce the appearance of undesirable secondary reactions that could modify the petrophysical properties of the studied rocks. All products were supplied by the company BLUESTAR-SILICONAS HISPANIA belonging to the group RHÔNE-POULENC.

The treatments were carried out as follows:

a. For aging, cubic samples (6 × 6 × 6) cm were submitted to 25 cycles of freezing/thawing and cooling/heating (− 20 to 110 °C) in a climatic chamber (Fig. 1) to simulate an artificial degradation under controlled conditions (Iñigo et al. 2000, 2001, 2006, 2013). The process to follow is as follows: after a drying period at 60 °C until constant weight was reached, the blocks were submerged in distilled water for 16 h (rocks are saturated), after which they were cooled to − 20 °C and kept at that temperature for 3 h. Following this, temperature was raised to 110 °C (rate = 2 °C/min), and the blocks were held at that temperature for 3 h. Finally, the blocks were left for 2 h at room temperature and the process was started again, Fig. 2. The objective of this test was to determine the durability of the treated and untreated quarry samples.
b. The consolidation treatments were carried out following a recommended procedure by Iñigo et al. (2006), using different concentrations of the consolidation products (ranging from 5 to 70% w/w in white spirit). Each sample was fully immersed in the consolidation solution to allow the product to enter inside the stone. Following application, the stone's surface was gently washed with white spirit several times to avoid the non-homogeneous distribution of the product on the external surface of the blocks, and curing was carried out at room temperature

Fig. 1 Climatic chamber

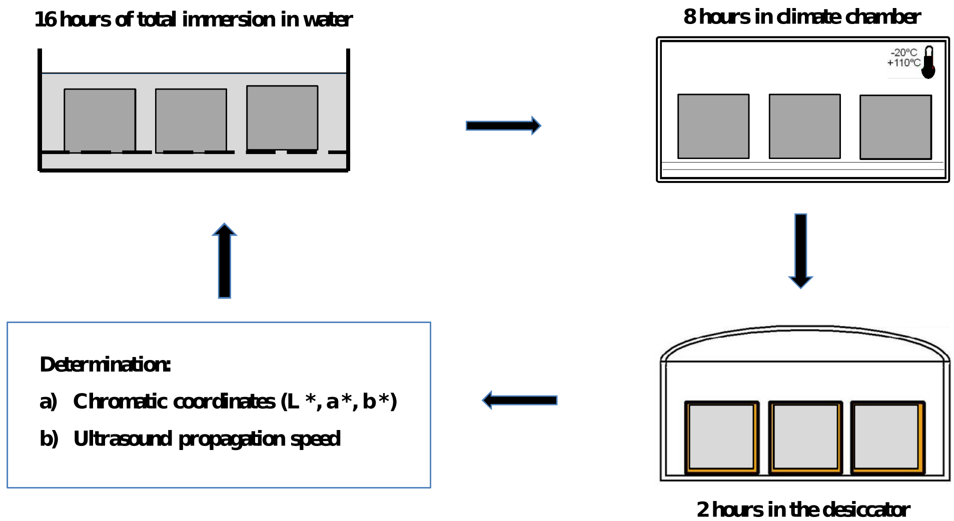

Fig. 2 Scheme for monitoring the cycles

for 1 month. The objective of this test was to determine the effectiveness of the consolidation treatments applied.

c. The hydrofuging treatment was carried out on the stone surface in two consecutive steps, 24 h apart, using a brush (Iñigo et al. 2001). The samples were left in ambient conditions for 2 weeks before measuring the color or any of the other properties studied (Iñigo et al. 2006). The objective of this test was to determine the effectiveness of the applied hydrofugation treatment.

Color was measured using a Minolta model CR-310 colorimeter specific to solid materials. The optical system of the measuring head contains a pulsed xenon arc lamp inside a mixing chamber, which provides diffuse and even lighting over the 50 mm diameter measuring area.

The Canonical Biplot, equivalent to the MANOVA analysis (Multivariate Analysis of Variance) was applied for carrying out the above-mentioned objectives (Grossi et al. 2015). This multivariate technique, which includes all the characteristics of the Biplot method (Gabriel 1971, 1972, 1975) used to discriminate the set of groups of previously established populations, was later developed and completed (Amaro et al. 2004; Galindo 1986; Vicente-Villardon 2018) and applied to the field of Cultural Heritage conservation (Iñigo et al. 2014, 2017, 2019; García-Talegón et al. 2016).

The results obtained are summarized on several factorial planes, where the variables are represented as vectors that begin at a hypothetical origin, and the means of the different groups represented as stars surrounded by confidence circles in the same reference system. The variables are highly correlated if two variables are represented by a very small angle, and their correlation is inverse if they are pointing in opposite directions. Additionally, if the angle is close to perpendicularity, their correlation is minimum. In the perpendicular projection of all the star markers onto the directions of any of the variables, the order of the projections in the direction of these variables is equivalent to the value that the means of the populations take for each variable. If two confidence circles are projected perpendicularly on one of the variables and the intervals of both projections do not overlap, this is tantamount to saying that there are differences between both means (Students' *t* test); the amplitudes of the circles will depend on the significance, α, determined (MSD, Bonferroni corrections, etc.). These interpretations are subject to a series of measurements of the quality of representation for the different planes (inertia absorption of the planes, the goodness of the projections of the measurements on the variables for the dimensions selected, etc.).

The Canonical Biplot analysis has been carried out on a matrix of 400 rows and 6 columns (L *, a *, b *, Vx, Vy, and Vz), where the rows are grouped into 40 groups with the following names: **STX**, where **S** is the type of quarry sample (**Z1, TG, TB, TO** and **TR**), and **TX** (00, T1, T2, T3, T4, T5, T6, and T7), where:

T0 = Quarry samples.

T1 = Quarry samples subjected to freezing/thawing and colding/heating (– 20/110 °C) accelerated aging.

T2 = Quarry samples treated with H224.

T3 = Quarry samples treated with RC70.

T4 = Quarry samples treated with RC80.

T5 = Quarry samples treated with H224 and subsequently subjected to freezing/thawing and cooling/heating (– 20/110 °C) accelerated aging.

T6 = Quarry samples treated with RC70 and subsequently subjected to freezing/thawing and cooling/heating (– 20/110 °C) accelerated aging.

T7 = Quarry samples treated with RC80 and subsequently subjected to freezing/thawing and cooling/heating (– 20/110 °C) accelerated aging.

A diagram of all the comparisons made in this study is shown in Fig. 3.

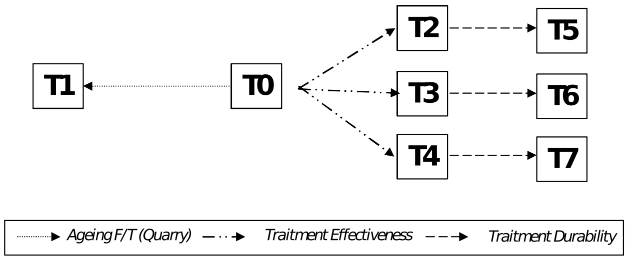

Fig. 3 Diagram of all the comparisons made in this study

The average data collected for each of the variables analyzed for each rock studied appear successively in Tables 1, 2, 3, 4, and 5.

The results obtained from the Canonical Biplot, Fig. 4, have been broken down for each of the samples studied to facilitate the interpretation of the results. This has given rise to Figs. 5, 6, 7, 8, and 9. Arrows with different paths have been introduced into these figures to graphically determine the approximate magnitude of the effects produced by the different processes applied. The significance of the effects was determined using *t*-Student comparisons (Bonferroni correction).

Table 1 Average data on the ultrasound propagation speed and the chromatic coordinates of sample Z1

Sample	Vx^f	Vy^f	Vz^f	L*	a*	b*
Z1T0	2376 ± 71	2315 ± 74	2124 ± 36	67.1 ± 0.5	2.2 ± 0.2	9.9 ± 0.4
Z1T1	2365 ± 93	2243 ± 121	2068 ± 136	73.4 ± 1.3	1.2 ± 0.1	8.5 ± 0.3
Z1T2	3209 ± 72	3153 ± 83	2891 ± 162	70.1 ± 0.4	1.4 ± 0.1	9.9 ± 0.1
Z1T3	3369 ± 26	3265 ± 53	3147 ± 26	68,5 ± 0.5	1.7 ± 0.1	9.3 ± 0.4
Z1T4	3862 ± 15	3363 ± 95	2824 ± 69	71.7 ± 0.4	1.0 ± 0.1	8.2 ± 0.1
Z1T5	3115 ± 80	2957 ± 90	2825 ± 100	69.1 ± 0.7	1.5 ± 0.1	8.3 ± 0.3
Z1T6	2771 ± 99	2400 ± 87	2348 ± 85	67.3 ± 0.5	2.1 ± 0.2	10.4 ± 0.4
Z1T7	3331 ± 55	2857 ± 144	2243 ± 23	71.6 ± 0.6	1.3 ± 0.2	7.6 ± 0.3

^{f}: m/s

Table 2 Average data on the ultrasound propagation speed and the chromatic coordinates of sample TG

Sample	Vx^f	Vy^f	Vz^f	L*	a*	b*
TGT0	2814 ± 54	2503 ± 66	2270 ± 51	72.0 ± 1.0	3.4 ± 0.7	10.7 ± 0.7
TGT1	1893 ± 33	1580 ± 1	1298 ± 15	69.0 ± 0.6	6.5 ± 0.6	11.6 ± 0.2
TGT2	2829 ± 7	2710 ± 7	2404 ± 3	63.6 ± 0.4	4.6 ± 0.2	15.8 ± 0.3
TGT3	2784 ± 10	2747 ± 17	2643 ± 4	60.4 ± 0.7	8.4 ± 0.8	14.8 ± 0.2
TGT4	2842 ± 26	2787 ± 15	2556 ± 59	63.4 ± 0.4	4.1 ± 0.3	14.2 ± 0.2
TGT5	2778 ± 1	2459 ± 46	2239 ± 72	61.2 ± 0.6	7.5 ± 0.6	14.1 ± 0.2
TGT6	2754 ± 31	2781 ± 31	2436 ± 14	66.5 ± 0.7	7.5 ± 0.6	14.1 ± 0.3
TGT7	2525 ± 8	2857 ± 17	2413 ± 4	65.4 ± 0.4	6.0 ± 0.4	13.5 ± 0.2

^{f}: m/s

Table 3 Average data on the ultrasound propagation speed and the chromatic coordinates of sample TB

Sample	Vx^f	Vy^f	Vz^f	L*	a*	b*
TBT0	2632 ± 64	2422 ± 56	2130 ± 32	79.3 ± 0.4	0.5 ± 0.1	6.0 ± 0.2
TBT1	2020 ± 95	1885 ± 82	1680 ± 62	78.3 ± 0.5	0.3 ± 0.1	6.6 ± 0.3
TBT2	2891 ± 11	2578 ± 22	2474 ± 31	76.5 ± 0.5	0.9 ± 0.1	8.4 ± 0.6
TBT3	2979 ± 30	2813 ± 7	2538 ± 13	69.0 ± 0.3	2.7 ± 0.1	8.4 ± 0.3
TBT4	2982 ± 4	2814 ± 32	2694 ± 54	71.4 ± 0.3	1.2 ± 0.2	8.9 ± 0.4
TBT5	2584 ± 36	2276 ± 58	2127 ± 40	73.7 ± 0.6	1.2 ± 0.1	9.5 ± 0.5
TBT6	2741 ± 84	2633 ± 83	2345 ± 73	70.6 ± 0.3	1.1 ± 0.1	10.2 ± 0.2
TBT7	2682 ± 64	2630 ± 76	2452 ± 120	70.7 ± 0.5	2.1 ± 0.1	10.1 ± 0.3

^{f}: m/s

Table 4 Average data on the ultrasound propagation speed and the chromatic coordinates of sample TO

Sample	Vx^f	Vy^f	Vz^f	L*	a*	b*
TOT0	2539 ± 50	2368 ± 48	2176 ± 43	72.0 ± 0.7	4.0 ± 0.4	12.7 ± 1.0
TOT1	2140 ± 3	1868 ± 58	1663 ± 6	70.9 ± 0.6	3.3 ± 0.4	13.1 ± 0.9
TOT2	2658 ± 3	2497 ± 8	2370 ± 9	68.8 ± 0.4	3.8 ± 0.3	16.6 ± 0.4
TOT3	2813 ± 1	2714 ± 11	2519 ± 17	62.2 ± 0.6	6.8 ± 0.6	16.4 ± 0.4
TOT4	2948 ± 19	2814 ± 25	2411 ± 12	69.0 ± 0.3	2.7 ± 0.1	8.4 ± 0.3
TOT5	2487 ± 1	2428 ± 7	2254 ± 50	66.2 ± 0.4	4.1 ± 0.3	14.1 ± 0.6
TOT6	2608 ± 10	2510 ± 24	2329 ± 10	67.6 ± 0.3	3.6 ± 0.3	16.3 ± 0.3
TOT7	2586 ± 11	2483 ± 10	2239 ± 15	65.5 ± 0.5	4.4 ± 0.3	15.0 ± 0.7

^{f}: m/s

Table 5 Average data on the ultrasound propagation speed and the chromatic coordinates of sample TR

Sample	Vx^f	Vy^f	Vz^f	L*	a*	b *
TRT0	2197 ± 34	2053 ± 38	1975 ± 54	79.3 ± 0.1	− 0.1 ± 0.1	9.9 ± 0.2
TRT1	1898 ± 63	1843 ± 47	1644 ± 15	73.9 ± 0.6	1.7 ± 0.4	10.7 ± 0.4
TRT2	2317 ± 9	2271 ± 1	2256 ± 4	66.0 ± 1.0	6.2 ± 0.9	14.5 ± 0.6
TRT3	2376 ± 13	2294 ± 22	2264 ± 20	64.9 ± 0.7	6.1 ± 0.8	14.2 ± 0.4
TRT4	2610 ± 15	2374 ± 14	2436 ± 21	63.3 ± 0.9	7.7 ± 1.1	16.6 ± 0.6
TRT5	2158 ± 25	1933 ± 9	1895 ± 22	75.8 ± 0.9	2.2 ± 0.9	10.9 ± 0.4
TRT6	2092 ± 92	2033 ± 75	1957 ± 63	74.5 ± 0.9	4.0 ± 0.9	11.7 ± 0.9
TRT7	2280 ± 45	2093 ± 1	1957 ± 12	68.3 ± 1.0	4.6 ± 0.9	12.4 ± 0.7

^{f}: m/s

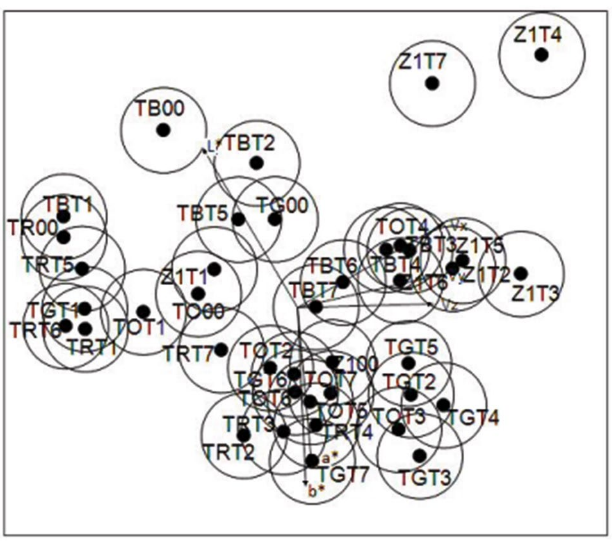

Fig. 4 Canonical Biplot (axes 1 and 2)

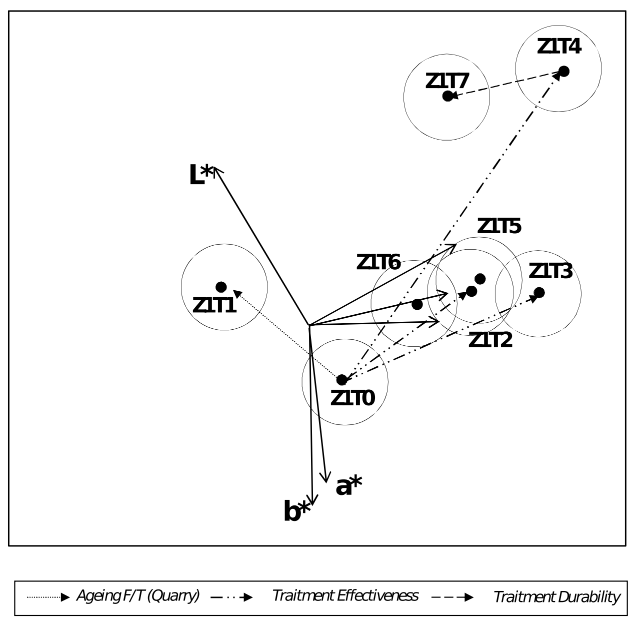

Fig. 5 Canonical Biplot for the stone variety Z1 (axes 1 and 2)

3 Results and Discussion

A Wilk's Lambda of 22.64 was calculated, $p < 0.0001$, after applying the Canonical Biplot to the results obtained for the chromatic coordinates (L *, a *, b *) and the ultrasound propagation speed. The inertia absorption of the first three axes was 87.66%.

The plane 1–2, as seen in Fig. 4, was analyzed, since it was possible to detect variations in the effectiveness of the treatments and the durability of the fresh and treated stones previously described. This plane was broken down according to the different sample types.

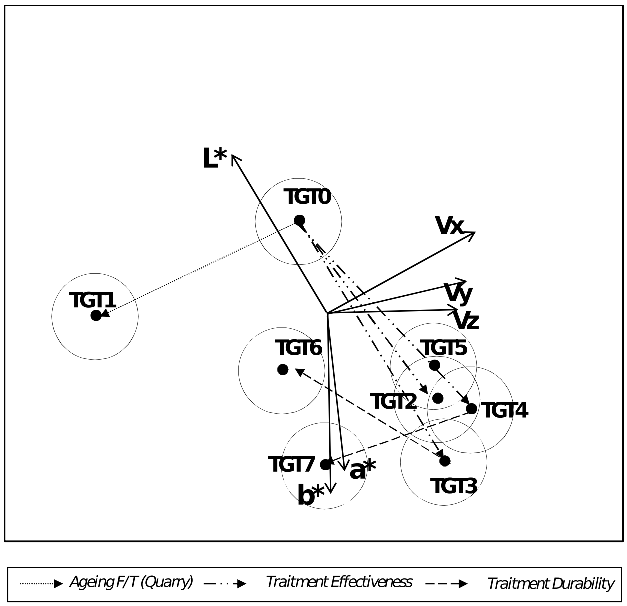

Fig. 6 Canonical Biplot for the stone variety TG (axes 1 and 2)

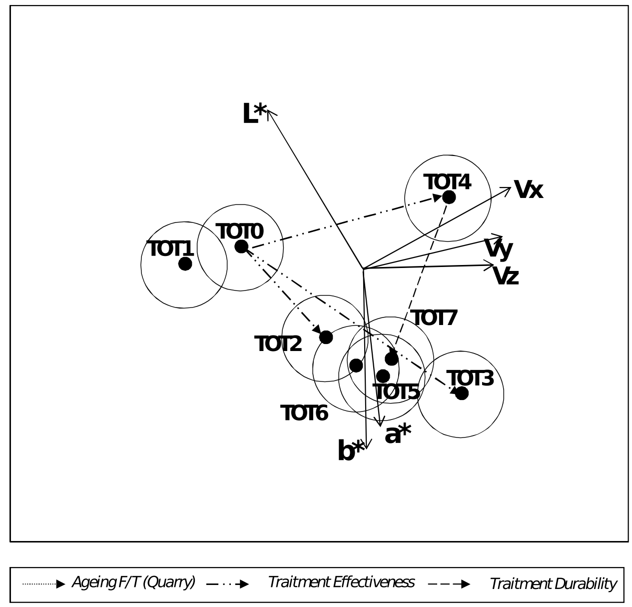

Fig. 8 Canonical Biplot for the stone variety TO (axes 1 and 2)

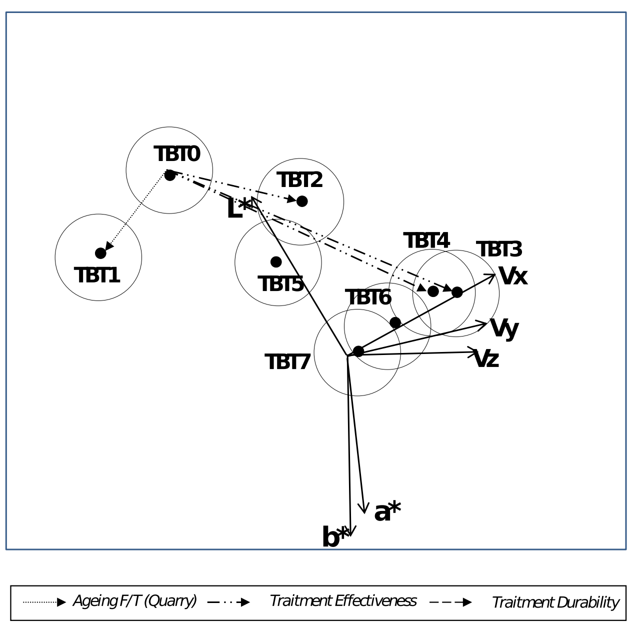

Fig. 7 Canonical Biplot for the stone variety TB (axes 1 and 2)

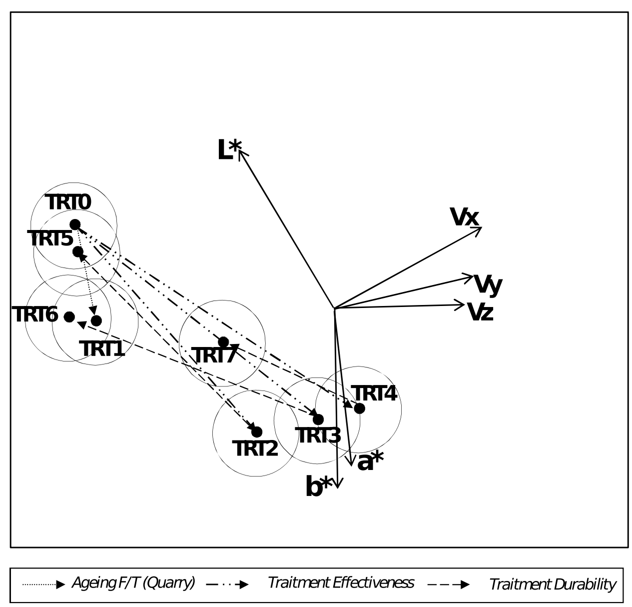

Fig. 9 Canonical Biplot for the stone variety TR (axes 1 and 2)

The results found are summarized in the following sections:

3.1 Durability of the Quarry Materials After Being Subjected to Freezing/Thawing and Cooling/Heating Accelerated Aging (– 20/110 °C)

The ultrasound propagation speed was lower for all of the treated samples when compared to the values obtained for the fresh, untreated quarry samples. However, in the case of samples, Z1 and TG differences were detected ($p < 0.05$). This decrease was due to the appearance of holes and microcracks inside the stones during aging using the freezing/thawing and cooling/heating (– 20/110 °C) treatments. The order in which this decrease was manifested was: TG > Z1 > TB ≈ TR ≈ TO, indicating that the greater the grain size of the minerals (TG and Z1), the greater the decrease in the ultrasound propagation speed. That is to say, the holes and microcracks open in the materials with a larger grain size were greater in the interconnective space between minerals. Additionally, no variations were observed in samples TB, TO, and TR, as these are the most porous stones with a large number of pores greater than 5 µm. The process of freezing/thawing did not cause a disruptive effect, because drainage occurred, as well as the expulsion of fluids within the advance line of the freezing front (Winkler, 1973).

In addition, the color of the stone variety Z1 was slightly lighter (↑ L*) ($p < 0.05$) as compared to the respective *fresh* quarry samples which were grayish white (Fig. 5). In the variety TR, a darkening occurred (↓ L*), as compared to the fresh quarry stone ($p < 0.05$), possibly due to the strong reddish color of its surface. In the chromatic coordinates that define color (a* and b*), samples TR and TG appeared redder (↑a^*) and more yellow (↑b*) ($p < 0.05$), whereas in sample Z1, the redness (↓a*) and yellowing (↓b*) ($p < 0.05$) decreased.

3.2 Effectiveness of the Treatments (H224, RC70, and RC80) Using Fresh Quarry Rocks

The ultrasound propagation speed was higher in all cases compared to the values obtained for the corresponding fresh quarry rocks ($p < 0.05$), except in sample TO treated with H224 (water repellent). This was due to how the product was originally applied, which did not produce a consolidating result but rather the formation of a thin film that acted hydrophobically. For this sample (TO), one of the most porous, it was more difficult to produce a hydrophobic film.

With respect to color, all of the treated, silicified sandstone samples (TG, TB, TO, and TR), as compared to the corresponding fresh quarry rocks appeared darker (↓ L*), with an increase in redness (↑ a*) and yellowing (↑ b*) ($p < 0.05$), except for the TB samples treated with H224 and the sample TO treated with RC80. The behavior of the treated silicified conglomerate (Z1) was, however, different; treatment with H224 produced less yellowing (↓ b*), but appeared lighter (↑ L*) and less yellow (↓ b*) and red (↓ a*) after being treated with RC80.

The extent of the effects produced allows us to approximate the effectiveness of the treatments applied. Therefore, in general, we can conclude that:

1. Treatment with H224 (T2) produced the least effect on all samples due to the way in which it was applied. Applying the product using a brush did not allow it to properly penetrate into the stone and to form a thin film that prevented water from entering.
2. In the case of the consolidation treatments RC70 (T3) and RC80 (T4), where maximum penetration was required, the effects were very similar, being more so with RC80.

3.3 Durability of the Treated Samples After Being Subjected to Freezing/Thawing and Cooling/Heating Accelerated Aging

Decreases in the ultrasound propagation speed were observed for all silicified sandstone samples previously treated and subsequently aged using freezing/thawing and cooling/heating (− 20/110 °C) treatments, as compared to the samples that were only treated with the conservation products ($p < 0.05$). However, this was not the case for sample TB, treated with all products, TO, treated only with H224 and RC80 and TG and Z1, treated only with H224.

There is a curious fact in the TR sample, Fig. 9. If we analyze the ultrasonic propagation speed, the conservation treatments used do not improve the durability of the treated stones compared to those of the fresh quarry samples, except in the samples treated with H224. This is due to the fact that the TR sample has the highest porosity of all those studied (Iñigo et al. 2020). This means that the consolidation products (RC70 and RC80) can be introduced in greater quantities and more easily into the interior of the rock. When performing the 25 aging cycles, the products can be eliminated by being easily dragged to the surface since most of their porosity is directly interconnected with the surface of the specimens (AC > 90%, Iñigo et al. 2020). The formation of the hydrophobic film (H224) is not as perfect and homogeneous as in the rest of the samples studied with less porosity. In spite of this, it seems that the stones of the TR sample, treated with this product, present a slightly higher durability compared to the corresponding quarry rocks, which is significant ($p < 0.05$) after the 25 cycles of accelerated artificial aging.

As for the color coordinate L*, no variations were detected ($p > 0.05$) for variety TB. In the variety TG, treated with RC70, and TR treated with all products (H224, RC70, and RC80), the stones became lighter in color (↑ L*); however, the behavior of sample TO treated with RC80 was darker (↓ L*) ($p < 0.05$). In addition, regarding the coordinates that define color, a* and b*, differences were only observed ($p < 0.05$) in TG, treated with RC70, and TR, treated with H224 and RC70. In these stone samples, the color was less yellow (↓ b*) and red (↓ a*), but in the case of TO, treated with RC80, the effect was the opposite.

Changes in the chromatic coordinates (L*, a*, b*) and the ultrasound propagation speed were greater when comparing the values of the treated samples with those obtained for the corresponding fresh quarry samples (), and when the fresh quarried samples () and the corresponding treated samples () are subjected to cycles of accelerated aging using freezing/thawing and cooling/heating treatments.

4 Conclusions

The analysis of the results obtained for the chromatic coordinates (L *, a *, b *) and the ultrasound propagation speed, in the three spatial directions of the different situations to which each of the silicified sandstones and conglomerates were subjected, by means of the Canonical Biplot analysis, has allowed us to draw the following conclusions:

a. Most of the variations found in all of the controlled non-destructive variables in this type of rock are obtained after the applying the treatments. In this study, the order of effectiveness of the conservation products applied is: RC80 > RC70 > H224.
b. The accelerated aging applied to the fresh quarry samples studied using freezing/thawing and cooling/heating (− 20/110 °C) treatments decreases the speed of ultrasound propagation in all cases. Additionally, the ultrasound propagation speed increases in the treated samples compared to fresh quarry samples. Finally, the ultrasound propagation speed is reduced, in general, in the samples treated and subsequently aged using a freezing/thawing and cooling/heating (− 20/110 °C) treatments, but many exceptions occur.
c. The changes in the chromatic coordinates (L *, a *, b *) are not greatly appreciable in all of the variables and treatments applied for each of the samples, except for the sample TR.
d. The changes observed in the ultrasound propagation speed variable, between the fresh quarry samples and those treated after aged using the freezing/thawing and cooling/heating treatment, indicate that the durability of the treated samples is greater than that of the fresh quarried stone. This indicates that, in most cases, the treatments are effective when using these types of stones.

Acknowledgements The authors are grateful for financial support for this work from the Ministry of Science and Innovation (MAT2010-20660) and Ministry of Science, Innovation and Universities (PGC2018-098151-B-I00).

References

Amaro IR, Vicente-Villardón JL, Galindo-Villardón MP (2004) ANOVA Biplot para arreglos de tratamientos con dos factores basado en modelos lineales generales multivariantes. Interciencia 29:26–32

Añorve M (1997) Valoración del deterioro y conservación en la piedra monumental. Monografía M-56, CEDEX, Ministerio de Fomento, Madrid

Aparecida-del Lama E, Kazumi-Dehira L, Grossi D, Kuzmickas L (2016) The colour of the granite that built the city of São Paulo. Brazil Color Resear Appl 41(3):241–245

Bellopede R, Manfredotti L (2006) Ultrasonic sound test on Stone: comparison of indirect and direct methods under various test conditions. In: Fort R, Alvarez-de Buergo M, Gomez-Heras M, Vazquez-Calvo C (eds) Heritage, weathering and conservation, vol 2. Taylor & Francis Group, London, pp 539–546

Carmona-Quiroga PM, Martínez-Ramírez S, Sánchez-de Rojas M, Blanco-Varela MT (2010) Surface water repellent-mediated change in lime mortar colour and gloss. Constr Build Mater 24:2188–2193

Castillo-Oli J (2018) La restauración de la Fachada Rica de las Escuelas Mayores de la Universidad de Salamanca. In: Azofra-Agustín E, Gutiérrez-Hernández AM (eds) Ex Vetere Novum Rehabilitar el Patrimonio Arquitectónico. Ediciones Universidad de Salamanca, Obra de referencia 42, Salamanca, pp 183–189

Chen TC, Yeung MR, Mori N (2004) Effect of water saturation on deterioration of welded tuff due to freeze–thaw action. Cold Reg Sci Technol 38:127–136

El-Gohary M (2013) Evaluation of treated and untreated Nubia sandstone using ultrasonic as a non-destructive technique. J Archaeol Sci 40(4):2190–2195

Gabriel KR (1971) The Biplot-graphic display of matrices with applications to principal component analysis. Biometrika 58:453–467

Gabriel KR (1972) Analysis of meteorological data by means of canonical decomposition and biplots. J Appl Meteorol 11:1071–1077

Gabriel KR (1975) MANOVA biplots for two-way contingency tables. In: Krzanowsky W (ed) Recent advances in descriptive multivariate analysis. Clarendon Press, Oxford, pp 227–268

Galindo MP (1986) Una alternativa de representación simultanea: HJ-Biplot. Qüestiió 1:13–23

García O, Rz-Maribona I, Gardei A, Riedl M, Vanhellemont Y, Santarelli ML, Strupi-Suput J (2010) Comparative study of the variation of the hydric properties and aspect of natural stone and brick after the application of 4 types of anti-graffiti. Mater Construcc 60(297):68–82

García-Talegón J, González-Sánchez M, Iñigo AC, Vicente-Tavera S, Rives V (2006) Microenvironments in the inner and outer parts of the Zamora Catedral. In: Fort R, Alvarez-de Buergo M, Gomez-Heras M, Vazquez-Calvo C (eds) Heritage, weathering and conservation, vol 1. Taylor & Francis Group, London, pp 457–461

García-Talegón J, Iñigo AC, Vicente-Tavera S (2013) Canonical Biplot as tool to detect microclimates in the inner and outer parts of Salamanca Cathedrals. In: Rogerio-Candelera MA, Lazzari M, Cano E (eds) Science and technology for the conservation of cultural heritage. Taylor & Francis Group, London, pp 59–62

García-Talegón J, Iñigo AC, Vicente-Palacios V (2016) A laboratory simulation of desalting on calcareous building stone with wet sepiolite. Environ Earth Sci 75:925–932

Grossi CM, Brimblecombe P (2008) Past and future colouring patterns of historic stone buildings. Mater Construcc 58(289–290):143–160

Grossi D, Aparecida-del Lama E, García-Talegón J, Iñigo AC, Vicente-Tavera S (2015) Evaluation of colourimetric changes in the Itaquera Granite of the Ramos de Azevedo Monument, São Paulo, Brazil. Int J Conserv Sci 6(3):313–322

Iñigo AC, Vicente-Tavera S (2001) Different degrees of stone decay on the inner and outer walls of a Cloister. Build Environ 36:911–917

Iñigo AC, Vicente-Tavera S (2002) Surface-Inside (10 cm) thermal gradients in granitic rocks. Effect of environmental conditions. Buil Environ 37:101–108

Iñigo AC, Vicente-Tavera S, Rives V, Vicente MA (1997) Colour changes in granitic materials surface by consolidated and/or water repellent treatments. Color Researc Appl 22(2):133–141

Iñigo AC, Rives V, Vicente MA (2000) Reproducción en cámara climática de las formas de alteración más frecuentes detectadas en materiales graníticos, en clima de tendencia continental. Mater Construcc 50:57–60

Iñigo AC, Vicente-Tavera S, Vicente MA, Rives V (2001) Effect of treatments on the pore network of granites. J Mater Civil Eng 13(3):166–168

Iñigo AC, Vicente-Tavera S, Rives V (2004) MANOVA-BIPLOT statistical analysis of the effect of artificial ageing (freezing/thawing) on the colour of treated granite stones. Color Resear Appl 29:115–120

Iñigo AC, Vicente-Tavera S, Rives V (2006) Statistical design applied to hydric property behaviour for monitoring granite consolidation and/or water-repellent treatments. Mater Construcc 56(281):17–28

Iñigo AC, García-Talegón J, Vicente-Tavera S, Martín-González S, Casado-Marín S, Vargas-Muñoz M, Pérez-Rodríguez JL (2013) Colour and ultrasound propagation speed changes by different ageing of freezing/thawing and cooling/heating in granitic materials. Cold Reg Sci Technol 85:71–78

Iñigo AC, García-Talegón J, Vicente-Tavera S (2014) Canonical Biplot statistical analysis to detect the magnitude of the effects of phosphates crystallization aging on the color in siliceous conglomerates. Color Res Appl 39(1):82–87

Iñigo AC, García-Talegón J, Vicente-Tavera S, Casado-Marín S, Martín-González S (2017) Multivariate analyses of soluble salts responsible for pathologies in granites of the Roman Aqueduct of Segovia, Spain. Int J Conserv Sci 8(1):59–66

Iñigo AC, García-Talegón J, Vicente-Palacios V, Vicente-Tavera S (2019) Canonical Biplot as a tool to detect microclimates in the inner and outer parts of El Salvador Church in Seville, Spain. Measurement 136:745–760

Iñigo AC, García-Talegón J, Vicente-Palacios V, Vicente-Tavera S (2020) Evaluation of effectiveness of silicoorganic treatments using hydric properties. Archaeol Anthropol Sci 12(4):86

Liu H, Niu FJ, Xu ZY, Lin ZJ, Xu J (2012) Acoustic experimental study of two types of rock from the Tibetan Plateau under the condition of freeze–thaw cycles. Sci Cold Arid Reg 4(1):21–27

Mahmoud AM, Ammar HH, Mukdadi OM, Ray I, Imani FS, Chen A, Davalos JF (2010) Non-destructive ultrasonic evaluation of CFRP–concrete specimens subjected to accelerated aging conditions. NDT&E Int 43:635–641

Martin J, Feliu MJ, Edreira MC, Villena A, Calleja S, Pérez F, Barros JR, Plaza F, Ortega P (2002) The original colour of the building facades from "El Pópulo" an old quarter of Cádiz. In: Galan E, Zezza F (eds) Protection and conservation of the cultural heritage of the Mediterranean Basin. Swets & Zeitlinger BV, Lisse, pp 649–653

Matsuoka N (1990) Mechanisms of rock breakdown by frost action: an experimental approach. Cold Reg Sci Technol 17:253–270

Minster J, Drdacky M, Jirovsky I, Kloiber M, Micka M, Slizkova Z, Vaclavik P (2006) Diagnostic techniques to assess mechanical characteristics of historical timber. In: Fort R, Alvarez-de Buergo M, Gomez-Heras M, Vazquez- Calvo C (eds) Heritage, weathering and conservation, vol 2. Taylor & Francis Group, London, pp 667–673

Molero M, Aparicio S, Al-Assadi G, Casati MJ, Henández MG, Anaya JJ (2012) Evaluation of freeze–thaw damage in concrete by ultrasonic imaging. NDT&E Int 52:86–94

Ortiz R, Ortiz P, Martín JM, Escudero C (2013) Analysis of heat effects due to fires on calcareous stones. In: Rogerio-Candelera MA, Lazzari M, Cano E (eds) Science and technology for the conservation of Cultural Heritage. Taylor & Francis Group, London, pp 139–142

Pelin V, Sandu I, Gurlui S, Brânzilă M, Vasilache V, Borş E, Sandu IG (2016) Preliminary investigation of various old geomaterials treated with hydrophobic pellicle. Color Researc Appl 41(3):317–320

Rivas T, Iglesias J, Taboada J, Vilán JA (2011) Sulphide oxidation in ornamental slates: protective treatment with siloxanes. Mater Construcc 61(301):115–130

Ruedrich J, Kircher D, Siegesmund S (2011) Physical weathering of building stones induced by freeze–thaw action: a laboratory long-term study. Environ Earth Sci 63:1573–1586

Sebastián-Pardo E, Zezza U (1998) Colour parameters of calcarenites used in the architectural heritage of the Andalusia (Spain) and Apulia-Basilicata (Italy). In: Castro-Castellano J (ed) Rehabilitación del Patrimonio Arquitectónico y Edificación. Centro Internacional para la Conservación del Patrimonio, CICOP, Tenerife, pp 560–572

Valdeón L, Montoto M, Esbert RM (1996) Tomography of the Axeitos Megalith (La Coruña, Spain): practical procedures and instrumentation. In: Vicente MA, Delgado-Rodrigues J, Acevedo J (eds) Degradation and conservation of granitic rocks in monuments. EUROPEAN COMMISSION, Brussels, pp 275–279

Vicente MA (1996) Granitic materials and historical monuments: study of the factors and mechanisms of weathering and application to historical heritage conservation. In: Vicente MA, Delgado-Rodrigues J, Acevedo J (eds) Degradation and conservation of granitic rocks in monuments. EUROPEAN COMMISSION, Brussels, pp 1–44

Vicente-Palacios V, Iñigo AC, García-Talegón J (2017) Multivariate Gaussian subspatial regression (MGSR) applied to predict the effect of phosphate crystalitation aging on the color in silicious conglomerates. Color Res Appl 42(6):799–806

Vicente-Villardón JL (2018) MULTBIPLOT: a package for Multivariate Analysis using Biplots. http://biplot.usal.es/ClassicalBiplot/index.html. Accessed 15 September 2018

Winkler EM (1973) Stone: properties, durability in man's environment. Springer-Verlag, Wien-New York, pp 28–159

Zezza F (2002a) Inland dispersion of marine spray and its effects on monument stone. In: Galan E, Zezza F (eds) Protection and conservation of the cultural heritage of the Mediterranean Basin. Swets & Zeitlinger BV, Lisse, pp 23–39

Zezza F (2002b) Non-destructive technique for the assessment of the deterioration processes of prehistoric rock art in karstic caves: the paleolithic paintings of Altamira (Spain). In: Galan E, Zezza F (eds) Protection and conservation of the cultural heritage of the Mediterranean Basin. Swets & Zeitlinger BV, Lisse, pp 377–388